

## VII. RADIO ASTRONOMY\*

Prof. A. H. Barrett  
Prof. J. W. Graham  
Prof. R. P. Rafuse  
A. T. Anderson III

V. J. Bates  
J. C. Blinn III  
R. A. Carreras  
V. K. Chung  
J. R. Cummings

J. R. Grindon  
R. J. Millman  
D. H. Staelin  
S. Weinreb

### A. MILLIMETER RADIO TELESCOPE

We now have under construction a radio telescope for use at millimeter wavelengths. A photograph of this facility, now on the roof of the Karl Taylor Compton Laboratories Building, is shown in Figs. VII-1 and VII-2. The mount, on loan to us from Lincoln Laboratory, is from a NIKE-AJAX tracking radar. We have had to make minor modifications, particularly in the servo controls, to accommodate our needs.

The parabolic reflector, manufactured for us by Antenna Systems, Inc., of Hingham, Massachusetts, is 10 feet in diameter and has a focal length of 4 feet. The reflector is an aluminum spinning filled with a plastic autobody filler that has been coated with a conductive surface that was applied after the plastic filler was machined to the precision surface. Measurements of the surface accuracy in the jig at the manufacturer's plant indicate tolerances within  $\pm .010$ " peak, with a large part of the surface within  $\pm .005$ ". If these dimensions are maintained on the mount, the facility should be usable at least to 100 kmc. A radiometric receiver at 4 mm is now under laboratory development. At this wavelength the antenna will have a beamwidth of  $\sim 0.1^\circ$  and a gain of approximately 63 db.

The NIKE-AJAX mount originally carried approximately 500 lbs load with a mechanical axis read-out accuracy of 0.1 mils ( $\sim 0.01^\circ$ ). The total weight of our reflector and its counterweight is approximately 1000 lbs, with approximately 575 lbs in the reflector and support and the remaining 425 lbs at the counterweight. It was necessary to offset the center of the reflector 1 foot from the center of the elevation axis to permit horizon coverage and yet clear the base of the mount. It is our intention to program the pointing of the antenna to  $\sim 0.01^\circ$  accuracy. Considerable care in accurate counterbalance and center of gravity control has been necessary to avoid unbalanced torques. Wind loads also contribute torque, but we hope to be able to maintain the  $0.01^\circ$  in winds of not greater than 20 mph. The main difficulty will be encountered in the elevation axis, since we do have only limited torque capability. Saturation torque is  $\sim 200$  ft-lbs.

The mount is controlled in azimuth and elevation coordinates. We wish to control the pointing in celestial coordinates, so a somewhat difficult coordinate conversion problem must be solved. Present plans include equipping the mount with azimuth and

---

\*This work was supported in part by the National Science Foundation (Grant G-13904); and in part by the National Aeronautics and Space Administration (Contract NaSr-101 and Grant NsG-250-62).

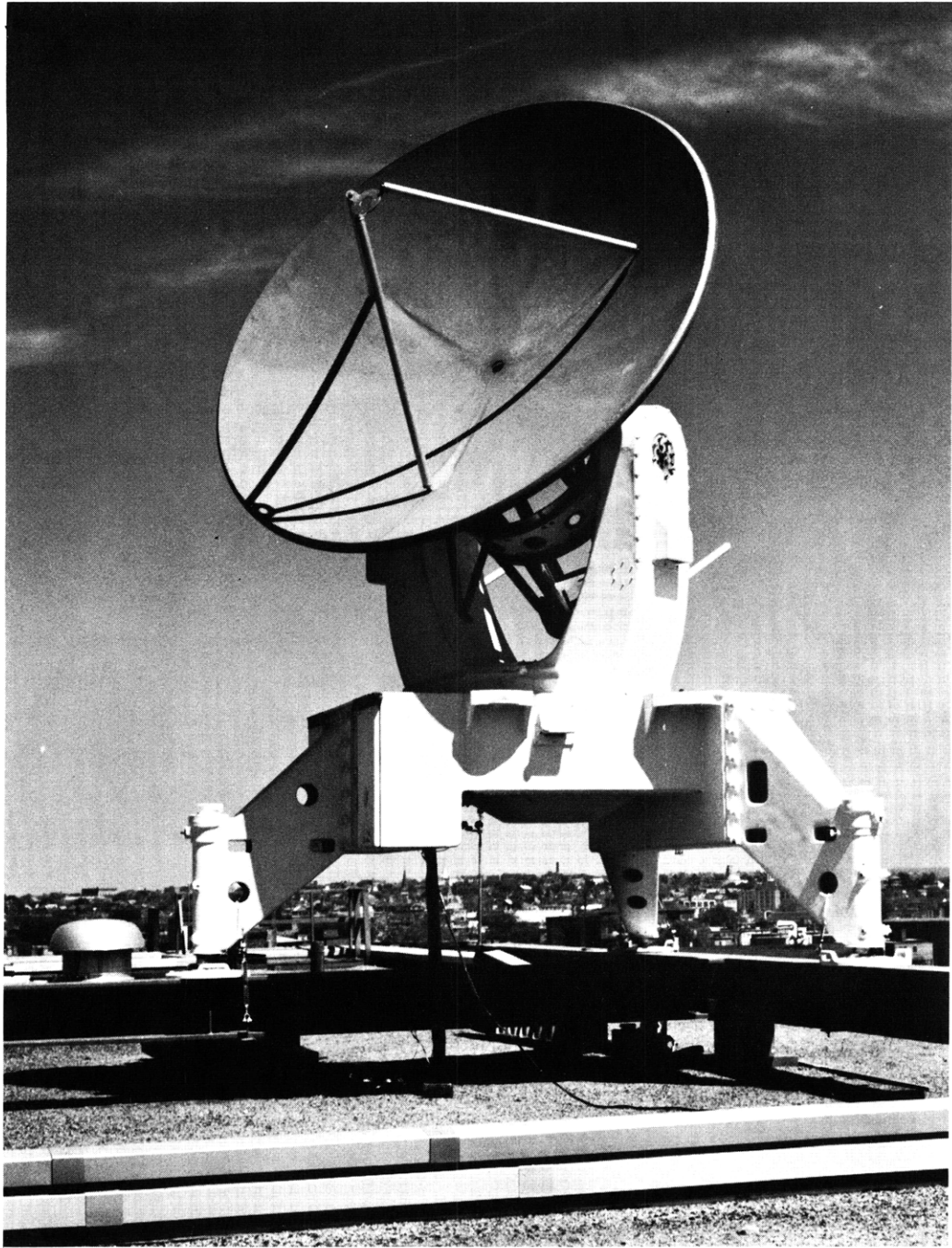


Fig. VII-1. Front view of millimeter radio telescope and NIKE-AJAX antenna mount.

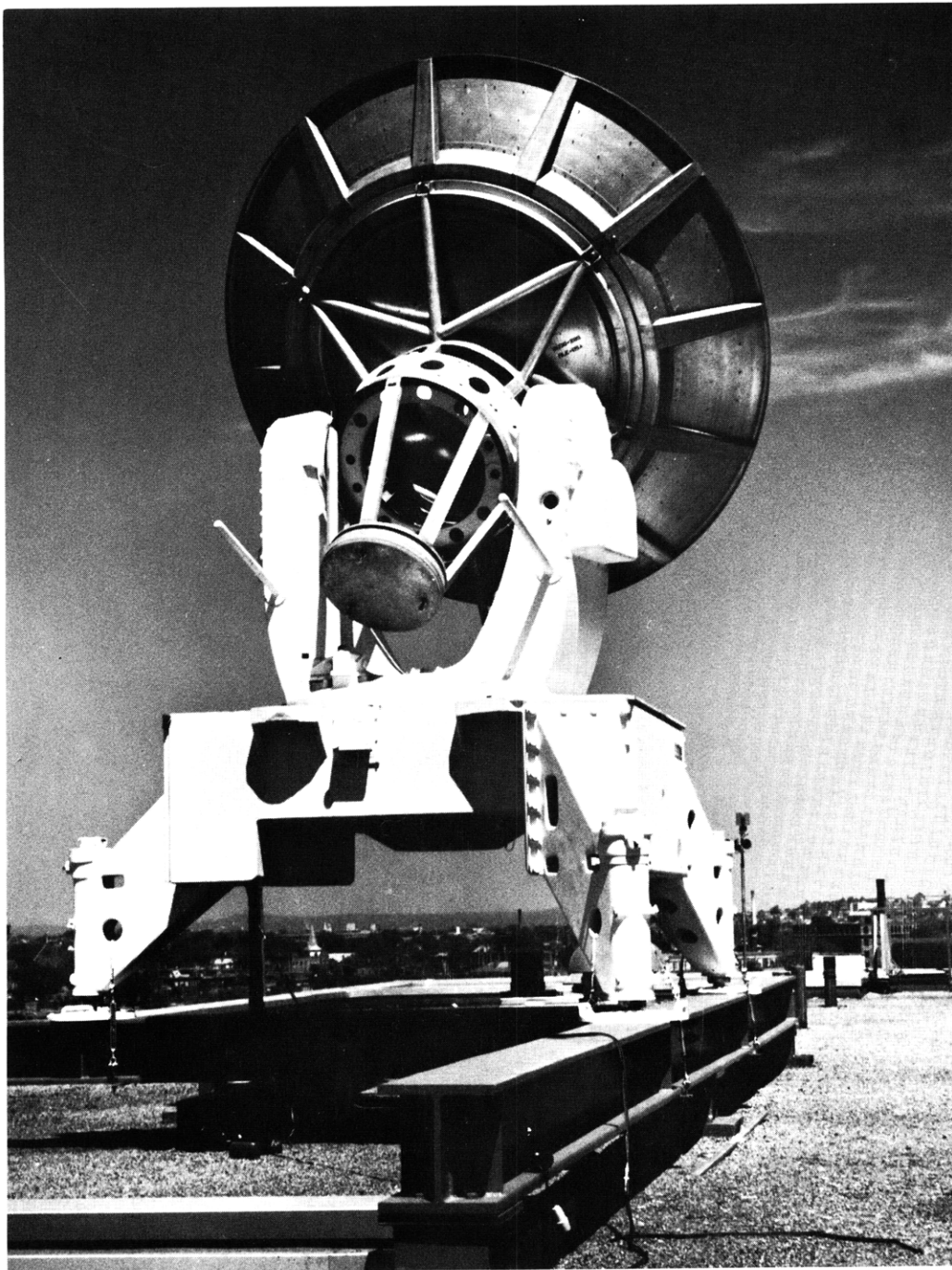


Fig. VII-2. Rear view of millimeter radio telescope showing offset counterweight.

## (VII. RADIO ASTRONOMY)

elevation digital read-outs and closing the angular-positional portion of the servo loops digitally by comparing the digital read-outs with azimuth and elevation information in digital form supplied by the PDP-1 digital computer that is available to our group. We plan to use the computer on a time-shared basis and to do extrapolation during a major portion of the time between computation of precise values of angles and angular rates. We are well into the computer program and hope to have the entire Digital Programmed Control of the radio telescope facility operating some time in the fall.

The immediate problem of major interest is to determine by experiment the actual pattern and gain of the parabolic reflector at millimeter wavelengths.

J. W. Graham

### B. ATMOSPHERIC WATER-VAPOR RESONANCE LINE PROFILE

Part of our program is directed toward a study of the terrestrial atmosphere at microwave frequencies. At wavelengths less than 1.5 cm the  $H_2O$  and  $O_2$  molecules of the atmosphere offer appreciable absorption to microwave radiation and numerous studies of this absorption have been carried out. However, such studies have been directed primarily toward determining the effect of  $H_2O$  upon propagation, and little attention has been paid to utilizing this effect as a means of studying the physical structure of the atmosphere. Toward this end, we have initiated a theoretical and experimental study of the resonance absorption line resulting from atmospheric  $H_2O$ , and we report here upon the results of the theoretical investigation.

The  $H_2O$  resonance line at 22,235 mc/l ( $\lambda = 1.35$  cm) has been well studied in the laboratory, therefore its absorption under conditions appropriate to the terrestrial atmosphere may be confidently predicted. The power-absorption coefficient  $a_1$  for a single resonance line may be written as

$$a_1 = \frac{8\pi^2 N |\mu|^2 \nu^2}{3ckT} \frac{e^{-E_5/kT}}{\sum_i e^{-E_i/kT}} f(\nu)$$
$$f(\nu) = \frac{\Delta\nu}{(\nu-\nu_0)^2 + (\Delta\nu)^2} + \frac{\Delta\nu}{(\nu+\nu_0)^2 + (\Delta\nu)^2},$$

where

$N$  = number of  $H_2O$  molecules per unit volume;

$\nu$  = frequency of the radiation;

$\Delta\nu$  = halfwidth of the line;

$\nu_0$  = resonant frequency;

$c$  = velocity of light;

$k$  = Boltzmann constant;

$T$  = atmospheric (absolute) temperature;

$E_i$  = energy of level  $i$ ; and

$\mu$  = dipole matrix element between the resonant states.

In addition to the line at 22,235 kmc,  $H_2O$  has many resonances at shorter wavelengths which exhibit absorption of the nonresonant type at microwave frequencies. The power-absorption coefficient for this absorption may be written as

$$a_2 = A \frac{N \nu^2 \Delta \nu}{T^{3/2}},$$

where  $A$  is a constant that is determined by the far infrared resonances.

In experiments of interest to us, the integrated absorption or optical depth is required. Formally, this can be written

$$\tau = \int (a_1 + a_2) dx,$$

where  $dx$  is an element of path length through the atmosphere. In general,  $dx$  is related to the altitude, the radius of the Earth, and the zenith angle of observation and becomes equal to the altitude only for a zenith angle of zero degrees. In performing the integration, suitable allowance must be made for the variation of temperature, pressure, and  $H_2O$  abundance with altitude, and we have incorporated the ARDC model of the terrestrial atmosphere for this purpose.<sup>1</sup>

The power per unit bandwidth  $P(\nu)$  radiated by the atmosphere is given by

$$P(\nu) = kT_A,$$

where

$$T_A = \int T e^{-\tau} d\tau.$$

The equations above enable predictions to be made of the power spectrum of the terrestrial atmospheric  $H_2O$  radiation. The variations of temperature and pressure with altitude are provided to sufficient accuracy by the ARDC model of the Earth's atmosphere; however, the distribution of  $H_2O$  in the atmosphere is neither accurately known nor constant. To show how the line profile is influenced by the vertical

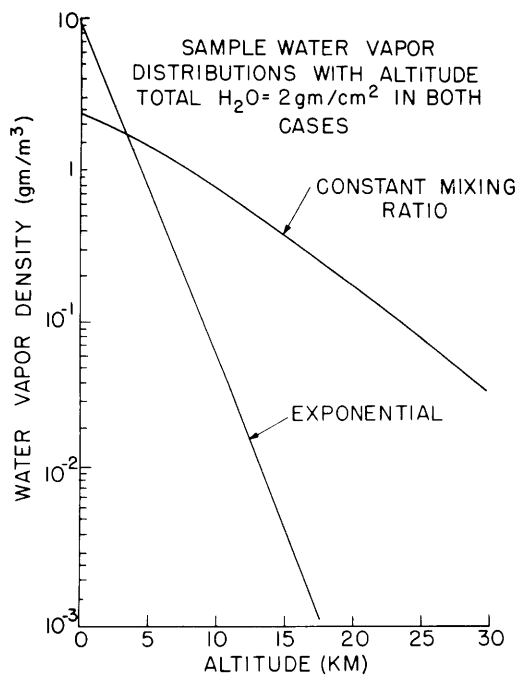


Fig. VII-3. Sample water-vapor distributions vs altitude. (In both cases total  $H_2O = 2 \text{ gm/cm}^2$ .)

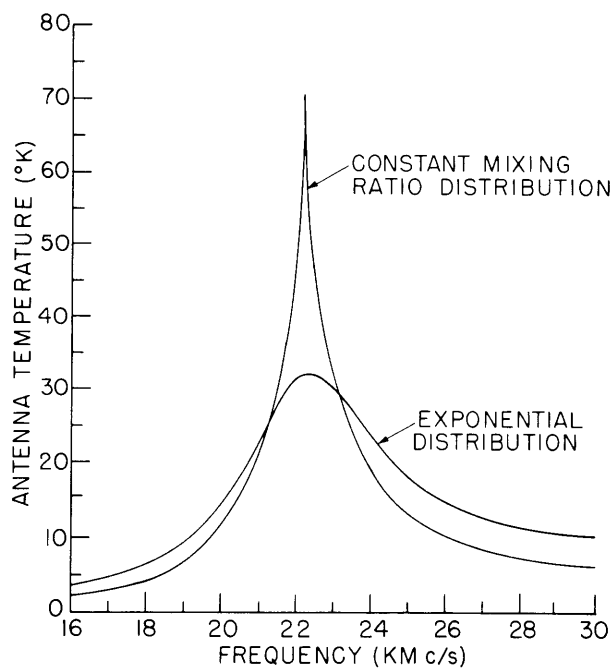


Fig. VII-4. Sample water-vapor resonance line profile. (Zenith angle,  $0^\circ$ .)

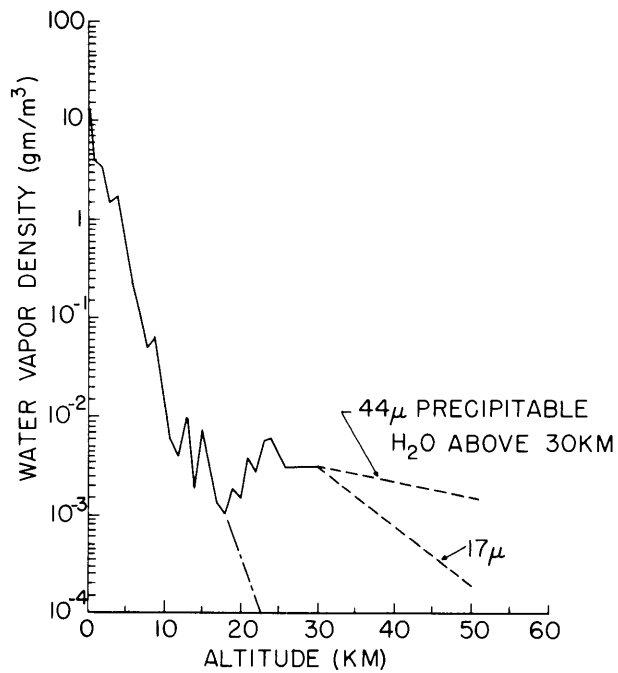


Fig. VII-5. Experimental water-vapor distribution (Barrett et al.<sup>2</sup>) normalized to 2 gm/cm<sup>2</sup> total H<sub>2</sub>O.

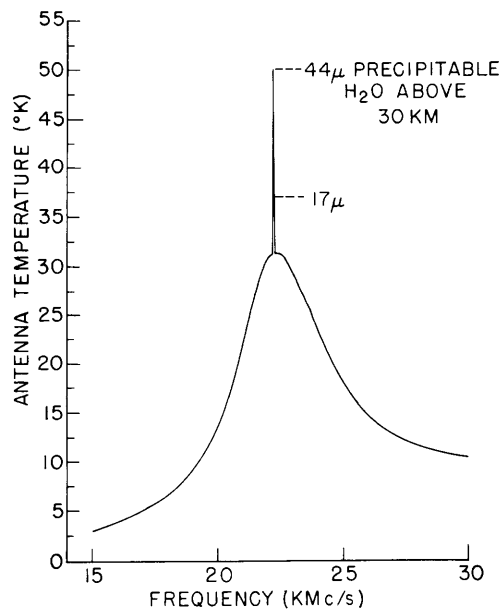


Fig. VII-6. Water-vapor resonance line profile based on experimental altitude distribution. (Zenith angle, 0 $^{\circ}$ .)

## (VII. RADIO ASTRONOMY)

distribution of  $\text{H}_2\text{O}$ , the expected profile was computed for the two distributions shown in Fig. VII-3. The total  $\text{H}_2\text{O}$  vapor in both cases is  $2 \text{ gm/cm}^2$ , and the resulting line profiles are shown in Fig. VII-4. These curves demonstrate how a detailed study of the line profile can be used to determine meteorological information.

An experimental determination of the  $\text{H}_2\text{O}$  distribution made from balloon observations is shown in Fig. VII-5. The abundance follows approximately an exponential distribution up to approximately 18 km, at which point it increases by a factor of approximately 5 up to 30 km, the maximum operating altitude of the balloon. Above this altitude, the total abundance was determined on two occasions to be  $17 \mu$  and  $44 \mu$  of precipitable  $\text{H}_2\text{O}$ . If the resonance line profile is computed by using this distribution, the results shown in Fig. VII-6 are obtained. It is seen immediately that the line shape resembles that obtained from an exponential distribution with the addition of a large contribution over a narrow frequency range because of the increased  $\text{H}_2\text{O}$  at high altitudes. Therefore it becomes possible to determine the amount of  $\text{H}_2\text{O}$  in the upper atmosphere from ground-based observations. Of particular importance will be temporal variations in the  $\text{H}_2\text{O}$  abundance on both short and long time scales.

The equipment for an experimental study of the  $\text{H}_2\text{O}$  line profile is being constructed, and verification of the theoretical computations is being made.

The calculations were carried out at the Computation Center, M.I.T.

A. H. Barrett, V. K. Chung

### References

1. United States Air Force, Handbook of Geophysics (Macmillan Company, New York, 1960).
2. E. W. Barrett et al., Tellus 2, 302 (1950).

## C. A NEW UPPER LIMIT TO THE GALACTIC DEUTERIUM-TO-HYDROGEN RATIO

The detection of the 21-cm hydrogen line, in 1951, created interest in the possibility of detecting a similar deuterium line at a wavelength of 91.6 cm. By comparing the strengths of the two lines, the galactic deuterium-to-hydrogen ratio,  $N_{\text{D}}/N_{\text{H}}$ , could be determined. This quantity is of astrophysical interest because it will give information about the composition and nucleogenesis of the interstellar medium.<sup>1, 2</sup>

There have been four previous attempts to detect the deuterium line, and all have given negative results.<sup>3-6</sup> The most recent of these, at Jodrell Bank, set an upper limit on  $N_{\text{D}}/N_{\text{H}}$  of 1/4000 in the direction of the Casseopeia radio source; this value is slightly higher than the terrestrial abundance ratio of 1/6700.

Our work has consisted of attempting to observe deuterium absorption in the Cas A



radio source. The 85-ft telescope of the National Radio Astronomy Observatory, at Green Bank, West Virginia, was used to track Cas A 12 hours a day for 9 weeks. The receiving system has been described elsewhere.<sup>7</sup> It incorporates two techniques: (a) The autocorrelation function of the signal is determined digitally and Fourier-transformed by a computer to give the power spectrum. Use of this method gives high stability and permits multichannel operation (the spectrum is measured at many frequencies during the same time interval). (b) The effective observation time is quadrupled by using four switched receivers to monitor both polarizations all of the time. It was thus possible to have 76.5 days ( $6.6 \times 10^6$  sec) of effective observation time, even though the antenna was in use only 68 days.

The sensitivity of the autocorrelation system has been investigated theoretically,<sup>8</sup> and also been checked by computer simulation. The rms deviation,  $\Delta T$ , of the spectral measurement is given by

$$\Delta T = \frac{2.1}{\sqrt{Bt}} T_{\text{tot}},$$

where  $B = 3.75$  kc is the frequency resolution of the measurement,  $t = 6.6 \times 10^6$  sec is the observation time, and  $T_{\text{tot}} = 2000^\circ$  is the total noise temperature referred to the receiver input. These values give  $\Delta T = .027^\circ$ .

The spectral dip,  $T_D$ , resulting from deuterium absorption, is given by

$$T_D = \tau_D T_p,$$

where  $T_p = 0.46 T_{\text{tot}}$  is the contribution to the receiver input arising from the background source, Cas A, and  $\tau_D$  is the deuterium optical depth in the angle subtended by the source.

The relation relating  $\tau_D$  to  $N_D/N_H$  which we have calculated differs from those given previously by Shklovsky<sup>9</sup> and Adgie.<sup>10</sup> The peak optical depth of either gas<sup>11</sup> is given by

$$\tau = \frac{hc^2}{8\pi k} \cdot \frac{A}{T_s f_o \Delta f} \cdot \frac{g_1}{g_1 + g_o} \cdot N,$$

where  $A$  is the spontaneous emission probability,  $T_s$  is the spin temperature,  $f_o$  is the line frequency,  $\Delta f$  is the Doppler-broadened linewidth,  $g_1$  and  $g_o$  are the statistical weights of the upper and lower states, and  $N$  is the total number of atoms per unit cross section in the two states. Calculating the ratio of these quantities for deuterium and hydrogen gives

$$\frac{\tau_D}{\tau_H} = 0.33 \frac{N_D}{N_H}.$$

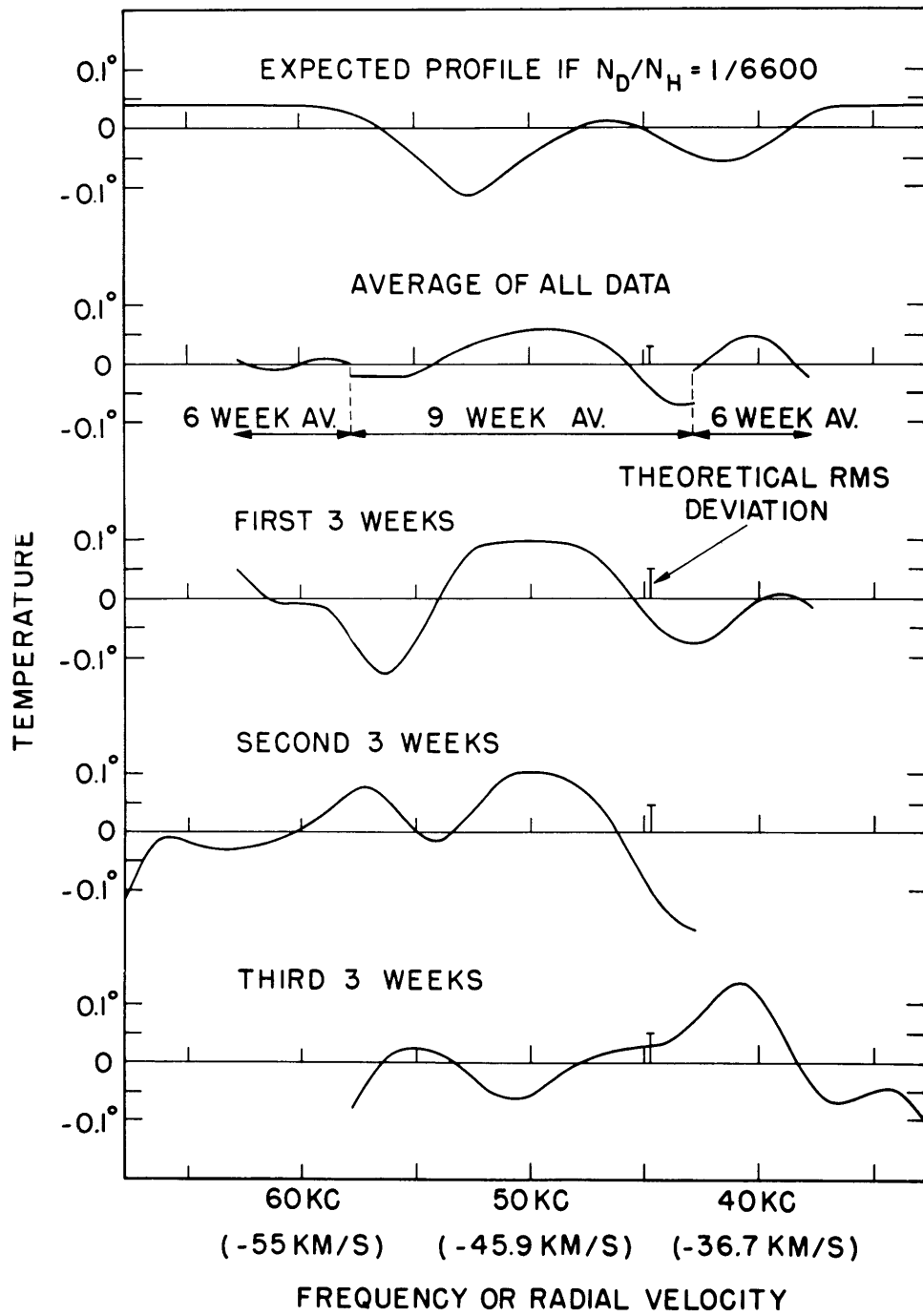


Fig. VII-7. Results of search for 327-mc deuterium line absorption in the Cas A radio source.

The following assumptions have been made:

(a) The value  $A_d = 4.65 \times 10^{-17} \text{ sec}^{-1}$  given by Field<sup>12, 13</sup> is correct, and the value  $6.6 \times 10^{-17} \text{ sec}^{-1}$  given by Shklovsky is incorrect.

(b) The ratio of the Doppler-broadened linewidths  $\Delta f_D/\Delta f_H$  would be equal to  $f_D/f_H$  if the atoms had the same rms velocities. However, approximately half of the broadening is due to thermal motion in which the deuterium atoms, having twice the mass, would have  $1/\sqrt{2}$  of the rms hydrogen velocity. Thus  $\Delta f_D/\Delta f_H = [1/2 + 1/(2\sqrt{2})] f_D/f_H$ .

(c) The spin temperatures for hydrogen and deuterium are assumed to be equal. Justification of this assumption is uncertain, since it depends on estimates of the intensity and detailed profile of the interstellar radiation field at the frequency of deuterium Lyman  $\alpha$  radiation.<sup>12</sup>

The value of the peak hydrogen optical depth in the Cas A radio source is also the subject of some controversy, its large value being difficult to measure. The first observers, Hagen, Lilley, and McClain,<sup>14</sup> using a 50-ft paraboloid, report  $\tau_H = 2.6$ . Muller,<sup>15</sup> using an 83-ft reflector, gives 4.0, and observers at California Institute of Technology,<sup>16</sup> using a single 90-ft telescope, report  $\tau_H > 4.7$ , and  $3.4 \pm .4$  when using two 90-ft telescopes as an interferometer. Accepting a value of peak hydrogen optical depth of 4, multiplying this by 0.8 to account for reduction because of the 3.75-kc bandwidth, and assuming a detection criterion of twice the theoretical rms fluctuation, we obtain a minimum detectable  $N_D/N_H$  of 1/18,000.

Our results are illustrated in Fig. VII-7. Individual 10-hour runs were examined for interference, corrected for any slope (typical slope correction,  $0.03^\circ/\text{kc}$ ), and averaged into 3-week lots. Examination of the 3-week averages indicates that the rms deviation is approximately 1.4 times the theoretical value, and thus the minimum detectable  $N_D/N_H$  should be raised to  $\sim 1/13,000$ . Our conclusion, then, is that the deuterium-to-hydrogen ratio in the region examined is, with probability 0.977, less than half of the terrestrial value.

S. Weinreb

#### References

1. L. Heller, *Astrophys. J.* 126, 341-355 (September 1957).
2. I. S. Shklovsky, *Cosmic Radio Waves* (Harvard University Press, Cambridge, Mass., 1960), pp. 257-260.
3. G. G. Getmanzev, K. S. Stankevitch, and V. S. Troitsky, *Doklady Akad. Nauk S.S.S.R.* 103, 783-786 (February 1955).
4. G. J. Stanley and R. Price, *Nature* 177, 1221-1222 (June 30, 1956).
5. R. L. Adgie and J. S. Hey, *Nature* 179, 370 (February 1957).
6. R. L. Adgie, *Paris Symposium on Radio Astronomy* (Stanford University Press, Stanford, Calif., 1958), pp. 352-354.
7. S. Weinreb, *Proc. IRE* 49, 1099 (1961).

## (VII. RADIO ASTRONOMY)

8. S. Weinreb, Internal Memorandum, Research Laboratory of Electronics, M.I.T., July 29, 1960.

9. I. S. Shklovsky, op. cit.; Equations 14-6, 15-4, 18-3, and 18-4 appear to be incorrect.

10. R. L. Adgie, op. cit., assumes that  $A_D/A_H = f_D^3/f_H^3$  and  $\Delta f_D/\Delta f_H = f_D/f_H$ . These assumptions are in error by small factors, Adgie's limit on  $N_D/N_H$  is more sensitive than he stated: 1/6400, instead of 1/4000.

11. J. P. Wild, *Astrophys. J.* 115, 206-221 (March 1952).

12. G. B. Field, *Proc. IRE* 46, 240-250 (1952).

13. This result has been computed independently by A. H. Barrett, Research Laboratory of Electronics, M.I.T.

14. J. P. Hagen, A. E. Lilley, and E. F. McClain, *Astrophys. J.* 122, 361-375 (November 1958).

15. C. A. Muller, *Astrophys. J.* 125, 830-834 (May 1957).

16. B. G. Clark, V. Radhakrishnan, and R. W. Wilson, Report No. 3, California Institute of Technology Radio Observatory, Pasadena, California, 1961.

### D. PROJECT LUNA SEE

In order to determine some of the possibilities of optical maser radar we conducted experiments with the Moon as a target. These experiments were made at Lexington, Massachusetts, on the evenings of May 9, 10, and 11, 1962.

#### 1. Predicted Performance

The basic system was conceived as consisting of a pulsed transmitter and a receiver. The transmitter was to be a ruby maser, radiating at  $6934 \text{ \AA}$ , and focused by a 12" reflecting telescope. The receiver was to be a photomultiplier tube illuminated by light collected in a 48" reflecting telescope. The photomultiplier output was to be displayed on a suitably delayed oscilloscope trace (the A-type of radar display).

If the light from the ruby were perfectly coherent over the cross section, and illuminated the 12" telescope uniformly, the beam divergence, given by  $\lambda/D$  would be  $\sim 2 \times 10^{-6}$  radians. Even allowing for a beam width 100 times greater, the resulting spot on the Moon, at a range of 200,000 miles, would constitute a point source for reradiation to the Earth. Thus, if we assume that the reflected light obeys Lambert's law, we get a modified "radar" equation, in which the received light energy  $W_R$  at the photocell varies as  $R^{-2}$  instead of as  $R^{-4}$ .

$$W_R = W_T \frac{A\rho}{\pi R^2} K_a^2 K_T K_R$$

where  $A$  is the area of the receiving aperture,  $R$  is the distance to the Moon,  $W_T$  is

(VII. RADIO ASTRONOMY)

the energy of the transmitted pulse,  $K_a$  is the transmission through the atmosphere,  $K_T$  and  $K_R$  are the optical efficiencies of the receiving and transmitting system, respectively,  $\rho$  is the normal albedo (reflectivity) of the lunar surface. We estimated (or knew) the constants of our system to have the following values:

$$A = 1 \text{ m}^2$$

$$K_T = 0.75$$

$$K_R = 0.37$$

$$K_a = 0.85$$

$$\rho = 0.15 \text{ (for a bright spot on the Moon)}$$

$$R = 384,000 \text{ Km}$$

and thus

$$\frac{W_R}{W_T} \approx 6.5 \times 10^{-20}.$$

If  $W_T = 50$  joules at  $\lambda = 6934 \text{ \AA}$ , there would be approximately 12.5 photons incident on the detecting photosurface per pulse.

Competing with our own signal are three noise sources: the dark current emitted by the photosurface, the ambient light from the lunar surface, and the light scattered in the atmosphere and the telescope. Manufacturer's data indicated dark currents for a cooled photomultiplier corresponding to approximately 10 photoelectrons per second. Since the maser pulse is of  $\sim 0.5 \times 10^{-3}$  sec duration, the expected received photon flux is of the order of  $2.5 \times 10^4$  photons per second. At  $6900 \text{ \AA}$  the efficiency of the photosurface is approximately 3 per cent, so that the expected signal component is  $\sim 750$  photoelectrons per second. Thus, the dark-current noise was expected to be negligible. At night, and aiming at the dark side of the Moon, the principal interfering sources are the Earthlight and the scattered light of the lunar crescent. The New Moon appears in the sky too early in the daytime, with a consequent high level of scattered light in the atmosphere. In addition the earthshine on the dark portion of the Moon is maximum at New Moon. Near Full Moon, the dark portion of the Moon is darkest, but the large amount of light scattered from the sunlit surface would make operation very difficult. The brightness of the dark side of the Moon varies approximately by a factor of 15 from just after New Moon to soon before Full Moon (a variation of  $100^\circ$  in phase).<sup>1</sup> From published data<sup>2</sup> it is estimated that, in the visible range, the power density incident on the Earth, reflected from the dark side of the Moon at First Quarter, is

## (VII. RADIO ASTRONOMY)

$$S = 3.3 \times 10^{-15} \frac{\text{watts/m}^2}{\text{km}^2 \text{ of Moon area}}$$

In a bandwidth of  $7 \text{ \AA}$ , centered at  $6934 \text{ \AA}$ , this corresponds to a power density of  $\sim 0.7 \times 10^{-17} \text{ watts/m}^2 \text{ km}^2$ , or approximately 28 photons/sec (meter)<sup>2</sup> (kilometer)<sup>2</sup>. Existing estimates of scattered light indicate an intensity from 1 to 10 times greater than this number.

The field of view of the receiving system was assumed to be limited by an aperture to an area on the Moon of  $\sim 5000 \text{ km}^2$ . Thus the background signal received by our  $1 \text{ m}^2$  telescope was expected to be approximately  $1.4 \times 10^5$  photons/sec because of Earth light, plus a component up to 10 times greater because of scattered light. Assuming  $5 \times 10^5$  photons/sec, and then including  $K_R$  and  $K_a$ , we find a "noise" flux of 160,000 photons/sec incident on the photocell. The maser pulse duration is  $\sim 1/2 \times 10^{-3}$  sec, and thus the expected background photon flux per pulse length would be approximately 80, and might be as low as 30.

These numbers indicate that the signal-to-noise ratio to be expected, for the parameters chosen, might be approximately 0.5, or less.

### 2. Description of the Apparatus

The telescope used for transmitting was a Cassegrainian reflector, focal length 4.55 m, aperture 0.29 m (12"). The maser unit, except for small modifications to the cooling system, has been described elsewhere.<sup>3</sup> Each of the four flashlamps is connected through a 0.3-mH choke to an 840- $\mu\text{F}$  bank of capacitors, charged to 2200 volts. In laboratory tests the output of the maser, as measured with a calorimeter, was observed to be approximately 50 joules. Since the cooling in the telescope installation had been improved in later tests, the actual radiated energy may have been somewhat greater. The maser beam is focused (Fig. VII-8) by a lens of 102-mm focal length onto the focal plane of the transmitting telescope. Measurements were made of the size of the focused spot by burning holes through an aluminum foil. The resulting holes had a diameter of approximately 0.9 mm. If the hole size is assumed to indicate the image size, the beamwidth radiated by the telescope is 0.2 mrad, maximum. The receiving telescope (Fig. VII-9) was also a Cassegrainian reflector of focal length 18.2 m and collecting area of  $1.00 \text{ m}^2$  (48" diameter).

A dichroic mirror was used to separate the red part of the spectrum so that the residual green light could be used for viewing through an eyepiece. The red part of the spectrum after  $90^\circ$  reflection by the mirror passed through a camera shutter and iris assembly at the focal plane, and was then collimated by a lens. The adjustable iris allowed us to modify the field of view accepted by the photomultiplier. Throughout the experiments the diameter of the circular opening of the diaphragm was 3.6 mm,

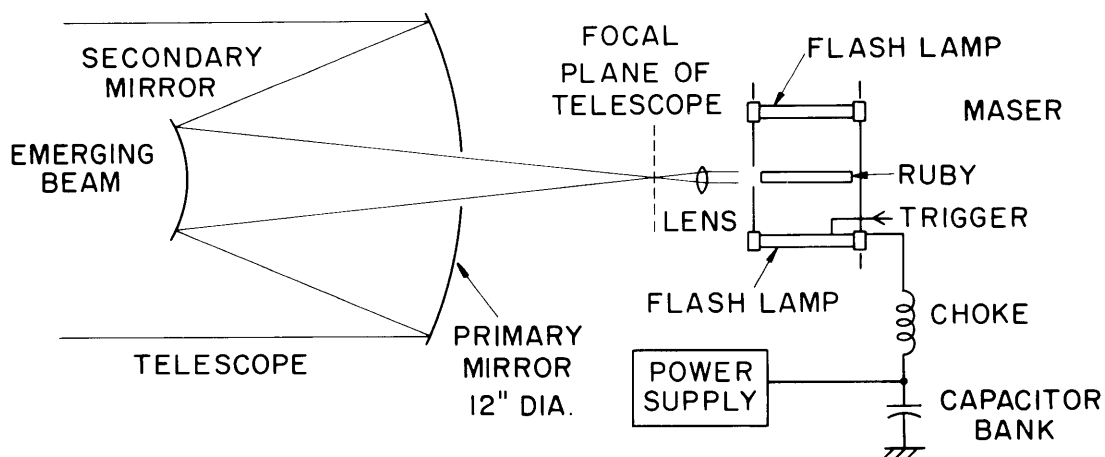


Fig. VII-8. Simplified diagram of the transmitter.

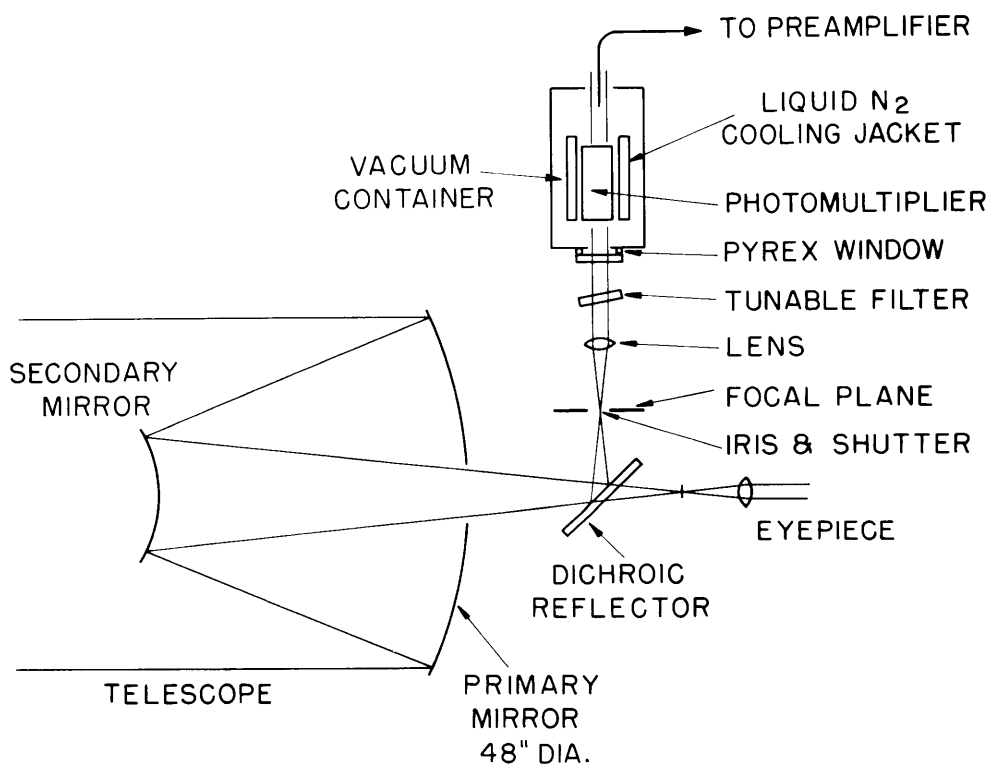


Fig. VII-9. Simplified diagram of the receiver. The interference filter was tuned by rotating its plane with respect to the optical axis of the system.

(VII. RADIO ASTRONOMY)

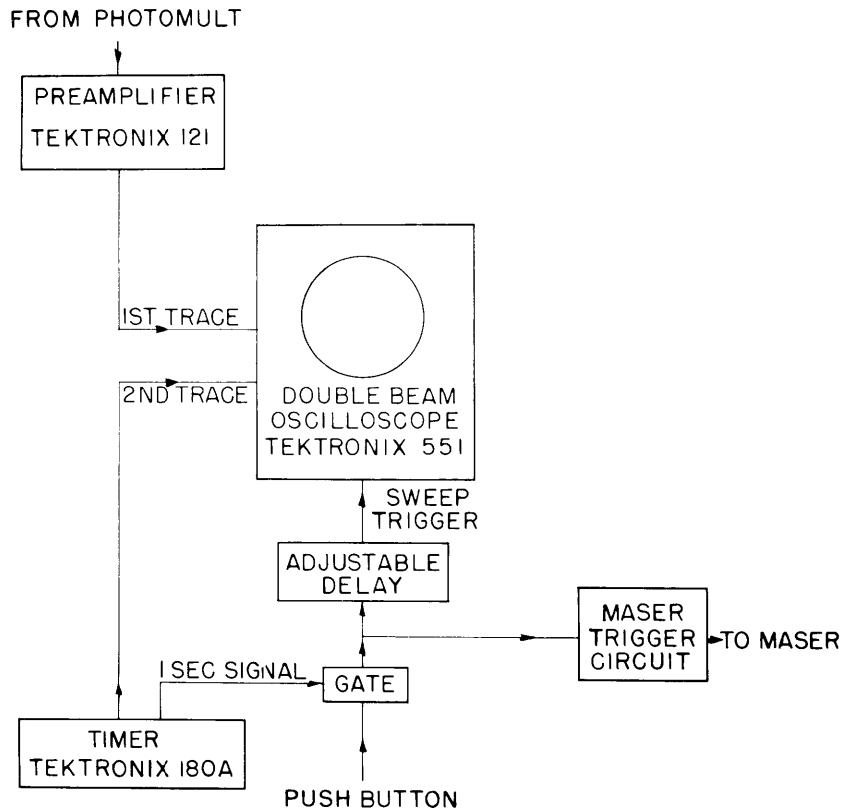


Fig. VII-10. Simplified diagram of control and display system.

equivalent to a field of view of 0.2 mrad. After going through the diaphragm and lens the red light passed through a combination of blocking filter and narrow-band tunable interference filter having a bandwidth of  $7 \text{ \AA}^4$ . The filtered light fell on the surface of an EMI 9558-A photomultiplier tube that was cooled to liquid-nitrogen temperature. The signals from the photomultiplier were preamplified and then displayed on one trace of a double-beam oscilloscope. In the second trace, timing signals from a Time Mark Generator were displayed. The 20-msec sweep was delayed approximately 2.6 seconds, differently on each night according to the Moon's distance. Each trace was photographed. The distance from Earth to Moon was computed from Ephemeris data.

In order to obtain accurate synchronization between the maser pulse and the delayed sweep, the circuit of Fig. VII-10 was used. The push button opened a gate in the firing circuit, but actual firing was initiated by a 1-sec repetition rate trigger pulse, derived from the timer. This trigger pulse also activated the delay oscilloscope sweeps.

### 3. Results

The experimental results are summarized in Table VII-1. The experiments are grouped in four series. The number of consecutive flashes in each series is given in



Table VII-1. Experimental results.

1	2	3	4	5	6	7
Eastern Standard Time	Region of the Moon	Number of Flashes	Number of Intervals	Average Noise	S. D.	Average Count in Expected Interval
9 May 62; 21 <sup>h</sup> 56-22 <sup>h</sup> 07	Albategnius 15°S 8°E	11	15	1.11	0.28	1.91
10 May 62; 21 <sup>h</sup> 52-22 <sup>h</sup> 34	Copernicus 10°N 20°W	23	16	1.39	0.22	1.74
11 May 62; 21 <sup>h</sup> 57-22 <sup>h</sup> 50	Tycho 43°S 10°W	30	22	1.42	0.16	1.83
22 <sup>h</sup> 54-23 <sup>h</sup> 15	Longomontanus 50°S 20°W	16	17	1.52	0.19	2.32

## (VII. RADIO ASTRONOMY)

column 3. Column 5 gives the average signal level (number of counts) obtained in a 0.5-msec interval, on account of Earth light and scattered light. The average was computed from actual counts in 0.5-msec intervals at time delays that were different from the expected round-trip time delay of the signal. Column 6 gives the standard deviation of the background level. The total number of intervals used in establishing the background is given in column 4. Column 7 gives the average photoelectron count obtained in that 0.5-msec interval where echoes were expected, and is therefore a measure of the signal plus noise.

It is evident that signal plus noise (column 7) exceeds the average noise by a significant amount in all experiments, but especially in the first and last ones. After completion of the experiments there were no signs of damage to the various optical elements of the transmitter. The focusing lens of the maser showed slight evidence of dust burned into the antireflecting coating.

We wish to acknowledge the help of J. Daley, Jr. of Lincoln Laboratory, M.I.T., in the adjustment and use of the telescope; of G. Hardway and S. Kass of the Raytheon Company, Waltham, Massachusetts, in the testing and use of the maser; and of G. McGrath of Lincoln Laboratory in computing the ephemeris data.

L. D. Smullin, G. Fiocco

### References

1. A. Danjon, Albedo, color and polarization of the earth, The Solar System, Vol. II, edited by G. P. Kuiper (University of Chicago Press, Chicago, Ill., 1954).
2. M. Minnaert, Photometry of the moon, The Solar System, Vol. III, edited by G. P. Kuiper and B. Middlehurst (University of Chicago Press, Chicago, Ill., 1961).
3. C. Bowness, D. Missio, and T. Rogala, A high energy laser using a multi-elliptical cavity, Letter to the Editor, Proc. IRE (to be published in July 1962 issue).
4. The filter was manufactured by Thin Film Products, Inc., Cambridge, Massachusetts.